Direct measurements of the ionospheric convection variability near the cusp/throat

S. G. Shepherd
Thayer School of Engineering, Dartmouth College, Hanover, New Hampshire, USA

J. M. Ruohoniemi and R. A. Greenwald
Johns Hopkins University Applied Physics Laboratory, Laurel, Maryland, USA

Received 2 May 2003; revised 21 August 2003; accepted 15 September 2003; published 11 November 2003.

[1] For the first time precise measurements obtained using Super Dual Auroral Radar Network (SuperDARN) radars are used to quantify the temporal variability in the convection velocity and identify the cause of the variations for a particular event located in the vicinity of the cusp. Using SuperDARN line-of-sight (LOS) Doppler velocities near 1200 magnetic local time and a standard fitting technique, the observed temporal variability is related to dayside convection features such as the cusp, convection throat, and convection reversal boundaries (CRBs). Two distinct regions of variability are observed: a region of high (often >500 m s^{-1}) hourly temporal variability occurring near the dayside CRB of the dusk convection cell during interplanetary magnetic field (IMF) $B_y < 0$, and a region of very low (<100 m s^{-1}) temporal variability in the convection throat. The source of the high variability near the dayside dusk CRB is caused primarily by motion of the large-scale convection pattern most likely due to the variable IMF. The line-of-sight velocities in this region fluctuate between sunward and antisunward directed flow depending on the position of the CRB relative to the radar observation area. In the convection throat, however, steady antisunward directed flow exceeding 500 m s^{-1} is observed despite the variable IMF. Based on these observations it is expected that increased Joule heating due to variability in the electric field occurs near the dayside CRB of the crescent-shaped convection cell and little additional Joule heating occurs in the convection throat. *INDEX TERMS:* 2411 Ionosphere: Electric fields (2712); 2427 Ionosphere: Ionosphere/atmosphere interactions (0335); 2437 Ionosphere: Ionospheric dynamics; 2463 Ionosphere: Plasma convection; 2736 Magnetospheric Physics: Magnetosphere/ionosphere interactions. **Citation:** Shepherd, S. G., J. M. Ruohoniemi, and R. A. Greenwald, Direct measurements of the ionospheric convection variability near the cusp/throat, *Geophys. Res. Lett.*, *30*(21), 2109, doi:10.1029/2003GL017668, 2003.

1. Introduction

[2] Variability of the convection electric field (or equivalently, the convection velocity) has been shown to be an important factor in calculating Joule heating rates in the upper atmosphere. General circulation models (GCM) of the thermosphere typically underestimate the magnitude of Joule heating when only the average electric field is included [*Codrescu et al.*, 1995]. Because Joule heating is proportional to the average of the square of the electric field, magnetospheric energy dissipation can be significantly increased when variability of the electric field is included in Joule heating calculations [*Codrescu et al.*, 1995, 2000].

[3] A complete characterization of the variability in the convection electric field would require simultaneous measurements of the field over the entire high-latitude ionosphere. Because such measurements are not possible, variability must be characterized by some other means. One method that has been used involves computing the sample standard deviations of the variances of electric field (or plasma drift) measurements from an empirical or statistical model. *Codrescu et al.* [2000] use this technique with incoherent scatter radar (ISR) drift measurements, while *Matsuo et al.* [2002] use plasma drift measurements from the Dynamics Explorer-2 (DE-2) satellite. Both studies result in bin-averaged maps of electric field variability that can be used with the average fields in Joule heating calculations.

[4] While characterizing electric field variability in a statistical sense is convenient for use with GCMs and results in enhanced Joule heating rates, it may not be the best method for understanding the dynamics and possible causes of the variability. It is, however, the only choice when using spatially localized measurements from a single satellite or ISR, or when the measurement uncertainties are large, as is typically the case with, for example, ISRs.

[5] If measurement uncertainties are low and available over extended regions, it is possible to characterize the variability in terms of the temporal variability, that is, by determining the amount of variation from a mean calculated from a set of measurements spanning a specified period of time. Characterizing variability in this manner is particularly useful in associating the observed variations with convection features often partially obscured by bin-averaged models. In some instances, as will be demonstrated, it is also possible to identify the direct cause of the variations.

[6] The focus of this study is on variations in the convection electric field which impact Joule heating rates. A 1-hr time scale is selected to emphasize variations that occur faster than the times typically required for the neutral atmosphere to respond to changes in the electric field through ion-neutral collisions [e.g., *Ponthieu et al.*, 1988]. Using line-of-sight (LOS) velocity measurements from the Super Dual Auroral Radar Network (SuperDARN) HF

0094-8276/03/2003GL017668$05.00

radars [e.g., *Greenwald et al.*, 1995], the temporal variability is determined as the weighted variance of the LOS deviations from a weighted hourly mean. The SuperDARN radars provide extended spatial measurements which are not only necessary for a non-statistical study, but are also useful for constructing maps of the large-scale convection pattern in order to interpret the variability measurements. These measurements of the temporal LOS velocity variability provide some insight into the processes which cause the observed variations that ultimately contribute to enhanced Joule heating rates.

2. Technique

[7] The standard SuperDARN radar mode sweeps sequentially through 16 different beam directions every 2 min to complete a single scan. The integration time for each beam is, therefore, ~7 s. The range resolution is set by the pulse width and is 45 km in the standard radar mode. A multipulse transmission sequence is used to determine a 17-lag autocorrelation function (ACF) at 70 distinct ranges. Each radar/beam/range is referred to hereafter as a range-gate. Standard processing (fitACF) renders estimates of the LOS velocity ($v_{\rm los}$) within each range-gate, and the associated error [*Villain et al.*, 1987; *Baker et al.*, 1988].

[8] The temporal variability for a particular range-gate is defined in this study as the weighted variance ($\hat{\sigma}_v$) of the deviations of the LOS velocities ($v_{\rm los}$) from a weighted mean ($\hat{\mu}_v$) over a 1-hr period. Specifically, the weighted mean ($\hat{\mu}_v$) of a set of N LOS velocity samples $\{v_{{\rm los}_i}\}$ and weights $\{w_i\}$ is given by:

$$\hat{\mu}_v = \left(\sum_{i=1}^{N} w_i^{-1}\right) \sum_{i=1}^{N} w_i v_{{\rm los}_i}, \qquad (1)$$

where each sample is assumed to be drawn from a Gaussian distribution with variance σ_i^2. The sample weight ($w_i = \sigma_i^{-2}$) is given by the uncertainty in the velocity ($v_{{\rm los}_i}$) determined by fitACF. The estimated weighted variance of the sample ($\hat{\sigma}_v$) is given by:

$$\hat{\sigma}_v^2 = \frac{\sum_{i=1}^{N} w_i}{\left(\sum_{i=1}^{N} w_i\right)^2 - \sum_{i=1}^{N} w_i^2} \sum_{i=1}^{N} w_i (v_{{\rm los}_i} - \hat{\mu}_v)^2 . \qquad (2)$$

[9] A further analysis of the $v_{\rm los}$ values can be performed to determine the large-scale convection pattern for each 2-min radar scan using the standard Johns Hopkins University Applied Physics Laboratory fitting technique [*Ruohoniemi and Baker*, 1998; *Shepherd and Ruohoniemi*, 2000]. These patterns allow the variability to be associated with features that may be responsible for the observed variations.

3. Observations

[10] A 1-hr period, 1742-1842 UT on 7 April 2001, was chosen for this study, in part, for the occurrence of extended SuperDARN backscatter in the high-latitude ionosphere, particularly near the cusp and convection throat. The extended observations were necessary to ensure an accurate determination of the large-scale convection pattern in the dayside region. During this day eight northern hemisphere SuperDARN radars were operating the standard radar mode, completing a scan every 2 min.

[11] Figure 1a shows $\hat{\sigma}_v$ calculated for the period 1742–1842 UT from the two SuperDARN radars looking into the convection throat, located at Kapuskasing, Ontario (KAP) and Saskatoon, Saskatchewan (SAS). The magnitude of $\hat{\sigma}_v$ is indicated by the color scale in the figure. Only ranges for which $v_{\rm los}$ was obtained for at least half of the 1-hr period are shown. Variability measurements from both KAP and SAS are shown in Figure 1a and generally agree, despite the different look directions of the radars. A convection map calculated using the gridded $v_{\rm los}$ data from all eight radars for the 2-min period starting at 1812 UT (the mid-point) is shown in Figure 1a.

[12] Figures 1b and 1c show expanded views of $\hat{\sigma}_v$ for each radar. Two range-gates are selected from each radar to illustrate the behavior of $v_{\rm los}$ over the entire 1-hr period in the two distinct regions. Time-series of KAP $v_{\rm los}$ data for beam and range (13, 33) and (10, 45) are shown in Figures 1d and 1e, respectively, while SAS $v_{\rm los}$ data for beam and range (13, 39) and (6, 39) are shown in Figures 1f and 1g, respectively.

[13] The time-series plots (Figures 1d–1g) all have the same format and scales. In these figures both the derived quantities obtained from fitACF and the raw spectra of the ACFs are plotted for each 7-s integration period at 2-min intervals. Each spectrum has been normalized to unity for comparison purposes. A solid red line is overlaid on top of each plot to indicate the values of $v_{\rm los}$ obtained from fitACF.

4. Discussion

4.1. Flow Near the Convection Reversal Boundary

[14] The velocity data shown in Figures 1d and 1f were collected from the vicinity of the sharp CRB feature in the dayside portion of the dusk convection cell. They show that the velocity variation was large (>1 km s^{-1}) and that this variability arose largely from switching between conditions of fairly stable sunward ($v_{\rm los} \sim 500$ m s^{-1}) and antisunward ($v_{\rm los} \sim -600$ m s^{-1}) directed flow. The implication is that within these fixed volumes the radars alternatively sampled flows from either side of the CRB, and that the velocity variability within the volumes arose largely from variability in the position of the CRB. The uncertainties in the velocity measurements were typically 10–50 m s^{-1}, i.e., much less than the magnitudes of the velocity jumps seen in Figures 1d and 1f. Thus it is safe to conclude that the plasma within these fixed volumes underwent sudden and large changes in velocity.

[15] Inspection of $v_{\rm los}$ data in sequential range-gates of several adjacent beams in the vicinity of the dusk CRB (not shown), show that the CRB is most often (1) well-defined by an abrupt transition from sunward to antisunward flow in a single range-gate (implying that the distance across the CRB is smaller than the 45 km range resolution) and (2) spatially extend over several hundred km (implying a large-scale feature). Previously reported

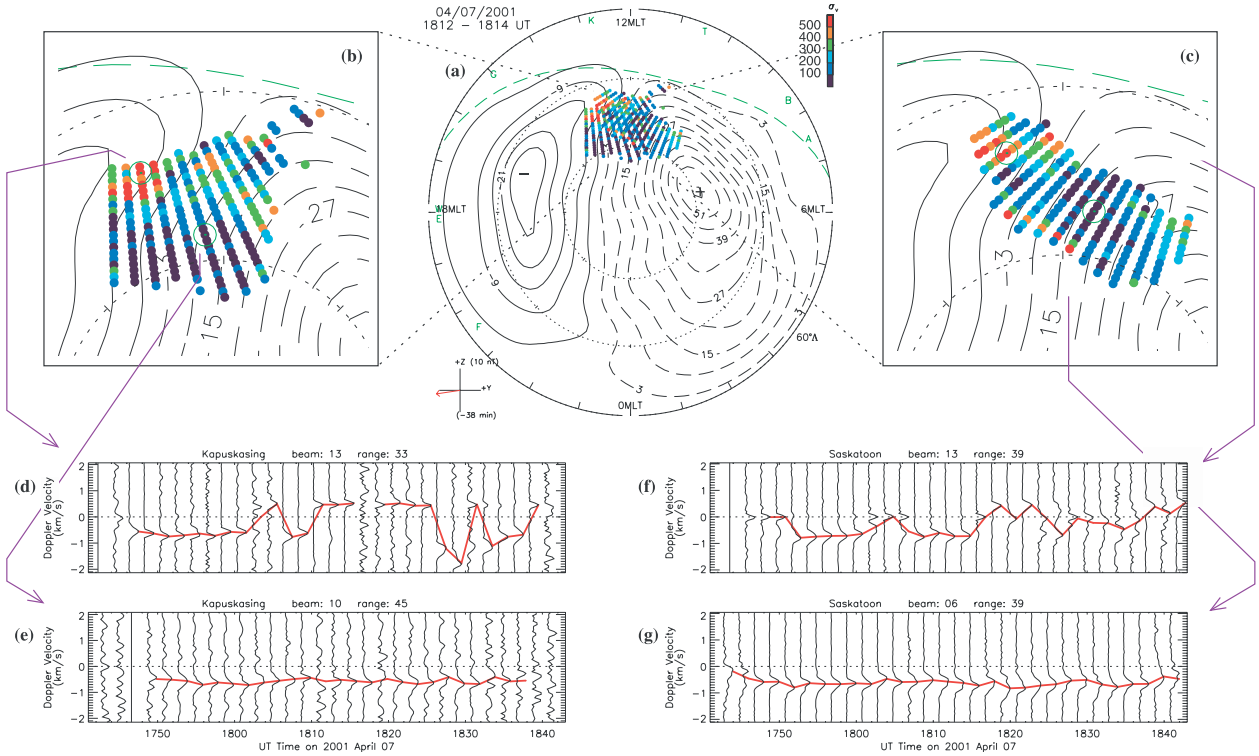

Figure 1. (a) 1-hr temporal variability map of the LOS Doppler backscatter from two SuperDARN HF radars in the cusp/throat region for the period 1742–1842 UT. Color indicates the degree of variability. A representative global convection pattern determined with the fitting technique of *Ruohoniemi and Baker* [1998] using data from all eight SuperDARN radars is shown for the period 1812–1814 UT. Expanded views of each radar are shown in (b) and (c). Time-series of raw spectra for the 1-hr period are shown for two representative range gates of each radar in (d)–(g). A red line indicates the LOS Doppler velocity determined from the fitACF procedure for each spectrum.

sources of localized CRB motion include ULF waves and traveling convection vortices [e.g., *Clauer and Ridley*, 1995; *Ridley and Clauer*, 1996]. Here we see that variations in the large-scale convection pattern can give rise to large velocity variations.

[16] Closer inspection of Figures 1d and 1f reveal that double-peaked (D-P) spectra are occasionally observed. The presence of multi-peaked spectra are most likely a consequence of variations occurring on scales smaller than those considered here. Other studies have looked at variability in the form of spectral width broadening of SuperDARN backscatter for even smaller scales than are considered here. These studies attribute broadened spectral widths in the cusp to small-scale vortices [*Schiffler et al.*, 1997; *Huber and Sofko*, 2000].

[17] It should also be emphasized that while the presence of D-P spectra can affect the degree of variability, depending on the relative power in the spectral peaks, the D-P spectra of the previous studies are of a very different character than those observed in Figure 1. The separation of peaks in the D-P spectra of previous studies were much smaller than the >1 km s^{-1} separations occasionally observed here. The large separation between sunward and anti-sunward directed flow clearly indicates proximity to the CRB in the occasional instances where D-P spectra are observed, rather than the presence of small-scale vortices. Large-scale motion of the CRB is otherwise observed.

[18] This result is not entirely unexpected. Data from the ACE spacecraft (not shown) show that while the pressure and IMF magnitude remain relatively constant for this period, the IMF orientation is quite variable. It is known from both theoretical studies of high-latitude convection [e.g., *Cowley and Lockwood*, 1992] and empirical models [e.g., *Ruohoniemi and Greenwald*, 1996] that variations in the IMF cause changes in the large-scale convection pattern, particularly near the dayside CRBs. The example reported here confirms that variability in the instantaneous convection pattern gives rise to localized and intense velocity fluctuations.

[19] It is expected that the variability will be larger in the dusk (dawn) convection cell for IMF with a dawn (dusk) component. The statistical models show that for dawn (dusk) directed IMF the dusk (dawn) cell is more crescent shaped and narrower on the dayside than the more round dawn (dusk) cell. Figure 1a shows that the convection pattern for this period is consistent with such a configuration for IMF $B_y < 0$. Any movement in the location of the dusk cell CRB will, therefore, result in more dramatic variations of v_{los} than would occur near the dawn cell CRB. This IMF B_y related asymmetry is seen in the statistical variability maps of *Matsuo et al.* [2003]. Their

result is confirmed by the case study presented here and, furthermore, the cause of the enhanced variability observed near the dayside CRB has been identified as resulting from motion of the CRB.

4.2. Flow in the Convection Throat

[20] In contrast to the highly variable flow near the dusk CRB, the flow in the convection throat is remarkably uniform and simple. The velocity data shown in Figures 1e and 1g were collected by the radars from a higher latitude region which was associated with fairly unstructured antisunward flow of $\sim$500 m s^{-1} throughout this period. The steady nature of the flow extends longitudinally for more than 1000 km and over 600 km in range (latitude), into the polar cap above 80° magnetic latitude, up to the far-range limits of the backscatter seen by the radars during this period.

[21] The temporal variability for the two range-gates in Figures 1e and 1g is <100 m s^{-1} and is representative of the general nature of the flow in this region. Any variability in the global convection pattern had little impact on the convection velocity in the poleward portion of the dayside convection throat. Accordingly, the variation in velocity was small compared to the variation encountered in the vicinity of the structured flows around the dusk CRB.

4.3. Joule Heating

[22] The importance of including a component of the electric field (**E**) due to small-scale or rapidly varying fluctuations in estimating Joule heating rates was demonstrated by *Codrescu et al.* [1995]. It is, therefore, expected that Joule heating will be pronounced in the vicinity of structure in the convection pattern, such as the CRB, especially in combination with variable behavior in the IMF. In the vicinity of the dusk CRB the Joule heating associated with the variable flow component ($\hat{\sigma}_v$ > 500m s^{-1}) is larger than that of the steady flow component ($\hat{\mu}_v \sim$ 200 m s^{-1}). By contrast, the variable component ($\hat{\sigma}_v$ < 100 m s^{-1}) is small compared to the steady component ($\hat{\mu}_v \sim$ 600 m s^{-1}) and makes only a small contribution to Joule heating in the high dayside convection throat.

[23] The situation is, of course, significantly more complicated than suggested here. The expression for the height-integrated Joule heating rate is often written as $Q_J = \Sigma_P \mathbf{E}'^2$, where Σ_P is the Pedersen conductance and $\mathbf{E}'$ is the electric field in the rest-frame of the neutrals [e.g., *Thayer*, 1998]. Upward field-aligned currents, for one, are likely to increase Σ_P and also contribute to enhanced Joule heating near the CRB. A complete treatment of Joule heating would require detailed knowledge of both the neutral winds and Σ_P.

5. Summary

[24] LOS Doppler velocities obtained from two SuperDARN HF radars looking into the cusp/convection throat have been analyzed to determine the 1-hr temporal variability in these data. Two distinct regions of variability and flow were observed during this period. A region characterized by large (>1 km s^{-1}) and rapid (<2 min) fluctuations in the LOS velocity is located near the dayside dusk CRB and another region at higher latitudes in the convection throat is characterized by relatively uniform flow over the polar cap at roughly 600 m s^{-1}.

[25] The velocity variations near the dusk CRB arise from motion of the CRB causing a fixed volume to alternately sample from sunward and antisunward directed flows. The dusk CRB is more favorable for large velocity variations than the dawn CRB owing to the sharpness of the reversal which is controlled by the IMF B_y orientation. The temporal variability near the dusk CRB is relatively high (often >500 m s^{-1}) while the variability of the uniform flow in the convection throat is low (typically <100 m s^{-1}).

[26] For the first time the origin of variability encountered in convection velocity on small temporal scales (2-min) has been shown. In this example the velocity within fixed volumes was observed to vary widely owing to the shifting position of structure in the convection pattern. The swings in velocity were large compared to the measurement uncertainties ($\sim$1 km s^{-1} versus $\sim$50 m s^{-1}). The highly variable velocities contrasted with the low variability within the region of unstructured flow.

[27] It is concluded that based on the work of *Codrescu et al.* [1995, 2000] and the observed velocity variability, Joule heating is likely to be pronounced in the vicinity of structured features of the convection, such as the CRB, especially in combination with variable behavior in the IMF. This study shows that variability of the convection pattern within the regions of structured flow is a significant factor for the coupling of energy from the magnetosphere to the ionosphere.

[28] **Acknowledgments.** This work was supported by NSF grant ATM-0202233. Operation of the Northern Hemisphere SuperDARN radars is supported by the national funding agencies of the U.S., Canada, the U.K., and France.

References

Baker, K. B., R. A. Greenwald, J.-P. Villain, and S. Wing, Spectral characteristics of high frequency (HF) backscatter from high-latitude ionospheric irregularities: Preliminary analysis of statistical properties, *Tech. Rep. RADC-TR-87-204*, Rome Air Development Center, Griffis Air Force Base, NY, 1988.

Clauer, C. R., and A. J. Ridley, Ionospheric observations of magnetospheric low-latitude boundary layer waves on August 4, 1991, *J. Geophys. Res.*, *100*, 21,873, 1995.

Codrescu, M. V., T. J. Fuller-Rowell, and J. C. Foster, On the importance of E-field variability for Joule heating in the high-latitude thermosphere, *Geophys. Res. Lett.*, *22*, 2393, 1995.

Codrescu, M. V., T. J. Fuller-Rowell, J. C. Foster, J. M. Holt, and S. J. Cariglia, Electric field variability associated with the Millstone Hill electric field model, *J. Geophys. Res.*, *105*, 5265, 2000.

Cowley, S. W. H., and M. Lockwood, Excitation and decay of solar wind-driven flows in the magnetosphere-ionosphere system, *Ann. Geophysicae*, *10*, 103, 1992.

Greenwald, R. A., et al., DARN/SuperDARN: A global view of the dynamics of high-latitude convection, *Space Sci. Rev.*, *71*, 761, 1995.

Huber, M., and G. J. Sofko, Small-scale vortices in the high-latitude *F* region, *J. Geophys. Res.*, *105*, 20,885, 2000.

Matsuo, T., A. D. Richmond, and D. W. Nychka, Modes of high-latitude electric field variability derived from DE-2 measurements: Emperical Orthogonal Function (EOF) analysis, *Geophys. Res. Lett.*, *29*(7), 1107, doi:10.1029/2001GL014077, 2002.

Matsuo, T., A. D. Richmond, and K. Hensel, High-latitude ionospheric electric field variability and electric potential derived from DE-2 plasma drift measurements: Dependence on IMF and dipole tilt, *J. Geophys. Res.*, *108*(A1), 1005, doi:10.1029/2002JA009429, 2003.

Ponthieu, J.-J., T. L. Killeen, K.-M. Lee, G. R. Carignan, W. R. Hoegy, and L. H. Brace, Ionosphere-thermosphere momentum coupling at solar maximum and solar minimum from DE-2 and AE-C data, *Physica Scripta*, *37*, 447, 1988.

Ridley, A. J., and C. R. Clauer, Characterization of the dynamic variations of the dayside high-latitude ionospheric convection reversal boundary and relationship to interplanetary magnetic field orientation, *J. Geophys. Res.*, *101*, 10,919, 1996.

Ruohoniemi, J. M., and K. B. Baker, Large-scale imaging of high-latitude convection with Super Dual Auroral Radar Network HF radar observations, *J. Geophys. Res.*, *103*, 20,797, 1998.

Ruohoniemi, J. M., and R. A. Greenwald, Statistical patterns of high-latitude convection obtained from Goose Bay HF radar observations, *J. Geophys. Res.*, *101*, 21,743, 1996.

Schiffler, A., G. Sofko, P. T. Newell, and R. A. Greenwald, Mapping the outer LLBL with SuperDARN double-peaked spectra, *Geophys. Res. Lett.*, *24*, 3149, 1997.

Shepherd, S. G., and J. M. Ruohoniemi, Electrostatic potential patterns in the high latitude ionosphere constrained by SuperDARN measurements, *J. Geophys. Res.*, *105*, 23,005, 2000.

Thayer, J. P., Height-resolved Joule heating rates in the high-latitude E region and the influence of neutral winds, *J. Geophys. Res.*, *103*, 471, 1998.

Villain, J.-P., R. A. Greenwald, K. B. Baker, and J. M. Ruohoniemi, HF radar observations of E region plasma irregularities produced by oblique electron streaming, *J. Geophys. Res.*, *92*, 12,327, 1987.

S. G. Shepherd (corresponding author), Thayer School of Engineering, Dartmouth College, 8000 Cummings Hall, Hanover, New Hampshire 03755-8000, USA. (simon.shepherd@dartmouth.edu)

R. A. Greenwald and J. M. Ruohoniemi, The Johns Hopkins University Applied Physics Laboratory, 11100 Johns Hopkins Road, Laurel, MD 20723, USA. (raymond.greenwald@jhuapl.edu; mike.ruohoniemi@jhuapl.edu)